

# FEMTOSECOND ELECTRON BUNCHES\*

Chitrlada Settakorn, Michael Hernandez, Kristina Woods and Helmut Wiedemann  
Stanford University, Stanford, CA 94309

## Abstract

Experiments to produce and measure femtosecond electron bunches are described. A 2.6MeV rf-gun with thermionic cathode is used at the SUNSHINE (Stanford UNiversity SHort INTense Electron Source) facility in conjunction with an  $\alpha$ -magnet for bunch compression to produce f-sec electron bunches. Transition radiation generated by these bunches is analyzed in a Michelson interferometer to determine the bunch length. Limitations on achievable bunch length and intensity will be discussed, as well as the technique used to measure such that bunches.

## 1 INTRODUCTION

Recently it has become possible to compress electron bunches to f-sec duration[1,2,3]. Development, use and understanding of such pulses become important for many research applications, such as, short wave length FELs, high energy linear colliders, generation of intense coherent far-infrared (FIR) radiation or radiolysis. At SUNSHINE we conduct such research with emphasis on generation and characterisation of f-sec electron bunches as well as their transformation to, and use of FIR.

## 2 FEMTOSECOND ELECTRON BUNCHES

Femtosecond electron bunches can be produced from an rf-gun with a thermionic cathode and a magnetic bunch compressor[1,6] The 2.6 MeV rf-gun consists of 1- $\frac{1}{2}$  cavities operating at 2856 MHz with a thermionic cathode attached to one wall of the first  $\frac{1}{2}$  cell as shown schematically in Fig.1.

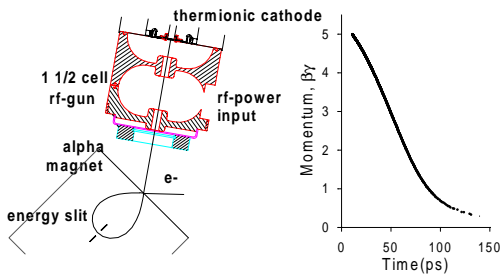


Figure 1: Rf-gun and  $\alpha$ -magnet with phase space distribution

Electron bunches from the rf-gun are then guided to an  $\alpha$ -magnet, in which the bunches are compressed down to 100 fs(rms). The beam enters the  $\alpha$ -magnet at an angle of  $49.29^\circ$  with respect to the magnet axis and follows an  $\alpha$ -like path, exiting again at the entrance point at a total deflection angle of  $278.58^\circ$  with respect to

the incoming beam. The electron bunches emerge from the rf-gun with a well-defined correlation between energy and time (Fig.1) such that higher energy particles are emitted first followed by lower energy particles. The increased path length for higher energy particles in the  $\alpha$ -magnet gives lower energy particles a chance to catch up for efficient bunch compression. In this process, 20 to 30 ps long bunches from the gun are compressed to less than 1 ps. After acceleration to some 30 MeV in a 3m single section S-band linac, the electron beam is guided to experimental stations.

Compression of electron bunches from such a rf-gun reaches a limit due to strong space charge forces and transverse emittance effects. At SUNSHINE the shortest achievable bunch lengths are limited by the transverse beam emittance. Particles with large transverse oscillation amplitudes in the focusing fields of quadrupole magnets travel a longer path than on-axis particles, thus lengthening the bunch length.

The electron beam is emitted in a train of about 3000 bunches each containing up to  $6.25 \times 10^8$  electrons or about 0.1nC. Highest peak currents of 306 A are reached for  $\sigma = 113$  fs.

## 3 BUNCH LENGTH MEASUREMENT

Bunch lengths well below one ps cannot be measured with electronic means anymore. A frequency domain method is therefore applied, utilizing FIR coherent transition radiation (TR) which is emitted when f-sec electron bunches pass through, for example, a thin Al foil. The radiation intensity scales like the square of the electron bunch population, reaching a level that can easily be detected with room temperature bolometers.

The spectral distribution of coherent TR is determined by the particle distribution in the bunch allowing the reconstruction of the bunch length. To characterize f-sec electron bunches from this radiation, we use a FIR Michelson interferometer in an autocorrelation set up as shown in Fig.2. The signal scan is the bunch autocorrelation function. The basic principle has been described elsewhere[1,4,5] and is briefly repeated here.

Coherent TR is generated when f-sec electron bunches pass through an Al foil tilted by  $45^\circ$  and the backward TR, emitted at  $90^\circ$  with respect to the beam axis, is extracted through a polyethylene window. In the Michelson interferometer, the radiation is split into two parts by the beam splitter. Each radiation pulse travels in different directions and is reflected by flat mirrors. A fraction of each beam then travels through the beam

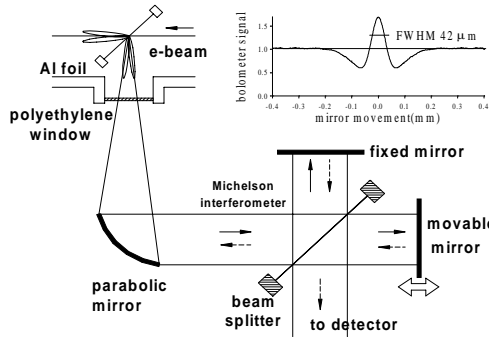


Figure 2: Michelson interferometer with a typical interferogram

splitter towards the bolometer. One of the mirrors is movable by a computer-controlled actuator. The bolometer signal recorded as a function of the mirror position or the optical path difference of both pulses, equal to twice the mirror movement, is called the interferogram. While the path length difference is larger than the bunch length, both radiation pulses arrive at the bolometer at different times. The bolometer detects the summation of both pulse energies independent of the path difference. As the path length difference becomes close to the bunch length, both pulses start to overlap and the radiation fields rather than energies add up, thus generating an increased signal detected by the bolometer. At equal path length, both pulses perfectly overlap, all radiation is directed toward the bolometer and its signal increased by a factor of two. The form of the interferogram in this overlap region resembles the particle distribution and ideally, the bunch length can be directly measured from the width of the interferogram. We also expect to extract from the interferogram and its Fourier transform, the spectrum, some information about the general particle distribution although such information is in principle lost in frequency domain measurements.

#### 4 DATA EVALUATION

Bunch length reconstruction is possible when most of the radiation spectrum is known. Therefore, we must evaluate the impact of frequency dependent effects in the measurement. Both the beam splitter and pyroelectric bolometer (Molecron P1-65) used at SUNSHINE display frequency dependent thin film interference effects. The spectrum is also affected by water absorption in a Michelson interferometer placed in ambient air.

The beam splitter is made of a Kapton foil which exhibits thin film interference effects at particular equidistant frequencies, depending on the foil thickness and index of refraction. The lack of reflection and therefore beam splitter efficiency at very low frequencies can greatly interfere with the determination of the bunch length measured. In a theoretical and experimental evaluation of this effect[4], it was found that the Kapton

beam splitter thickness must be equal to at least 1/3 of the bunch length for this interference effect to be negligible. For thick beam splitters the bunch length can be obtained directly from the central peak width (FWHM measured in terms of optical path difference), while for thinner beam splitters, increasing corrections must be applied. At SUNSHINE we use beam splitters of 12.5 to 125  $\mu\text{m}$  thickness. The correction required for a Gaussian beam is shown in Fig.3 displaying a correlation between interferogram width and bunch length.

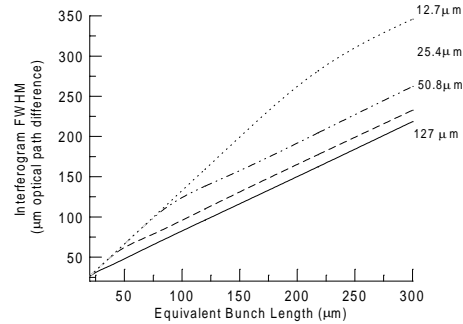


Figure 3: Interferogram FWHM's as functions of bunch length for different Kapton beam splitter ( $n=1.85$ ) thickness

The interferometer becomes particularly simple to construct and operate if it can be set up in air, however, causing water vapor absorption and dispersion. This effect was studied by comparing interferograms measured in air and in vacuum. Interferograms for both cases are shown in Fig.4, displaying clearly the increased interferogram width measured in air being consistently observed about 17 % wider than measurements made in vacuum. Including beam splitter corrections for the 25.4  $\mu\text{m}$  beam splitter used here, the bunch length measured in air is about 24% longer than measured in vacuum. We believe this broadening is due to dispersion rather than due to narrow water absorption lines. For precise measurements, either the interferometer must be placed under vacuum or corrections must be applied.

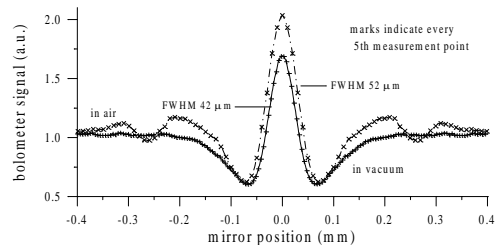


Figure 4: Interferogram measured in air and vacuum

The absorbing material of the bolometer is a 100  $\mu\text{m}$  thick  $\text{LiTaO}_3$  crystal which ideally would absorb all incident radiation. In reality, however, only a fraction is absorbed while the rest is reflected from the front and back surface. At unequal optical path lengths, part of the pulse from one arm may, after reflection on the back surface on the crystal, interfere with the later pulse from the longer arm. This leads to either increased or

decreased reflection from the bolometer as evident from the appearance of satellites in the interferogram (Fig.5). From the appearance of several satellites in the scan, we conclude that interference can occur after one or more reflections of the first pulse from the back surface. We believe that this interference effect does not affect the determination of bunch length because the basic shape of the spectrum is still preserved (Fig.5(b)). More research is required on this issue.

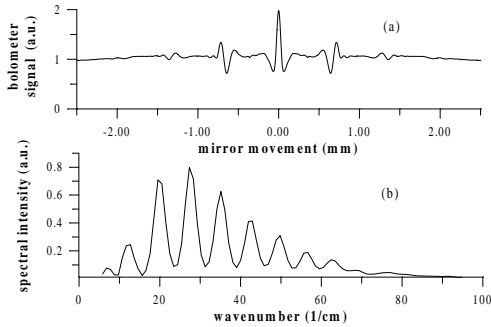


Figure 5: Bolometer interference effects on interferogram and spectrum.

## 5 PARTICLE DISTRIBUTION

The width of the interferogram peak resembles directly the effective bunch length; yet, the particle distribution is less well defined in this frequency domain observation. Particular features of an interferogram, however, correlate with features of the particle distribution. For example, a triangular interferogram results from an autocorrelation of a rectangular pulse and a Gaussian interferogram corresponds to a Gaussian pulse. We are particularly interested in distinguishing between a rectangular and a Gaussian distribution. To do this, the vicinity of the peak is probed in very short intervals. The interferogram exhibits a very rounded peak as expected for a Gaussian rather than a rectangular distribution. We are able to get further information from the derived spectrum. In Fig.6, the comparison of the spectrum with that of a Gaussian and a rectangular bunch including the beam splitter effect is shown.

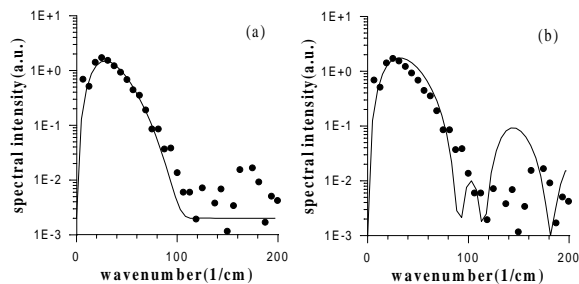


Figure 6: Radiation spectrum with a Gaussian(a) and the rectangular fit(b).

The measured spectrum agrees much better with a Gaussian distribution than a rectangular one. Specifically the increase in the intensity around  $150 \text{ cm}^{-1}$

wavenumber for a rectangular distribution is not observed. However, the best Gaussian fit is obtained for a bunch length of  $100 \text{ }\mu\text{m}$  rather than the  $84 \text{ }\mu\text{m}$  obtained from the interferogram. This discrepancy can be resolved if the particle distribution consists of a short  $84 \text{ }\mu\text{m}$  core and a Gaussian tail. Fig.7 shows the fit for this assumption assuming an  $84 \text{ }\mu\text{m}$  core with a  $150 \text{ }\mu\text{m}$  tail. For comparison, we show also a rectangular core with the same tail. We have no independent measurement to verify the existence of the tail, but are encouraged to this interpretation by confirming results from numerical beam simulation. Subjecting the measurement spectrum to a Kramers-Kronig analysis[7] again confirms the existence of a tail. Measuring the width of the interferogram at half height, as we do, does not include the effect of a tail which would show up only on the lower part.

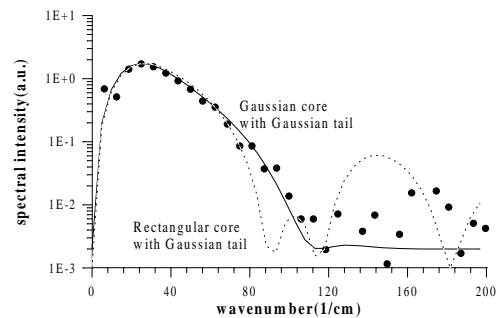


Figure 7: Radiation spectrum comparing with Gaussian and rectangular spectrum fit

## 6 CONCLUSION

Femtosecond electron bunches are generated and studied at SUNSHINE. The bunch lengths as short as  $113 \text{ fs}$ (rms) are measured using an autocorrelation of the coherent TR. Frequency dependent effects in the measurement are evaluated to avoid erroneous results and to extract more information on bunch distribution. Both interferogram and spectrum allow us to derive consistent bunch length measurements and some determination of particle distribution.

## 7 REFERENCES

- [1] P. Kung, D. Bocek, H. Lihn, H. Wiedemann, Phys. Rev. Lett. **73**(1994)967
- [2] M. Uesaka et al., J. of Nucl. Mats. **248**(1997)380-385
- [3] B.E. Carlsten et al., Phys. Rev. E **53**(1996)2072
- [4] H.C.Lihn, D. Bocek, P. Kung, C. Settakorn, H. Wiedemann. Phys. Rev. E **53**(1996)6413
- [5] C. Settakorn, M.Hernandez, H.Wiedemann, Proc.17<sup>th</sup> IEEE PAC97, Vancouver, B.C., Canada(1997)
- [6] H. Wiedemann, J. of Nucl. Mats. **248**(1997)374-379
- [7] Gi. Schneider et al., NIM A **396**(1997)283

\* Worked supported by DOE contract DE-AC03-76SF00515